Mathematics

https://www.aimspress.com/journal/Math

AIMS Mathematics, 10(4): 7891–7905.
DOI: 10.3934/math.2025362
Received: 06 December 2024
Revised: 19 March 2025
Accepted: 26 March 2025
Published: 03 April 2025

Research article

A numerical method using Legendre polynomials for solving two-point interface problems

Min Wu[1], **Jiali Zhou**[2], **Chaoyue Guan**[3] **and Jing Niu**[3,*]

[1] School of Science, Zhejiang University of Science and Technology, 310023 Hangzhou Zhejianag, China

[2] School of Mathematical Sciences, Zhejiang University of Technology, 310023 Hangzhou Zhejianag, China

[3] School of Mathematical Science, Harbin Normal University, 150025 Harbin Heilongjiang, China

* **Correspondence:** Email: njirwin@163.com.

Abstract: This paper presents a novel numerical algorithm that integrates reproducing kernel functions with Legendre polynomials to effectively address multiple interface problems. We create a new set of bases within the reproducing kernel space, introduce a linear operator, and utilize its properties to derive an equivalent operator equation. The model equation is then transformed into a matrix equation, enhancing the solution process for complex interface issues. Comparative numerical examples demonstrate the superior accuracy of our method over conventional approaches. Furthermore, the solution's existence and uniqueness are validated, ensuring the algorithm's reliability and effectiveness.

Keywords: Legendre polynomials; multiple interface problems; reproducing kernel method; linear operator
Mathematics Subject Classification: 41A10, 46E22

1. Introduction

In the field of mathematical physics, issues like heat transfer and electric field variations across different substances result in boundary value problems. These problems pertain to the resolution of elliptic differential equations that have discontinuous coefficients, which are commonly denoted as interface problems. Countless real-world phenomena can be encapsulated by elliptic equations with discontinuous coefficients. Take materials science, for instance; the connection of two materials with distinct conductivity properties is a typical scenario where such equations come into play. Moreover, in seepage mechanics, complex geological structures or multiphase fluids give rise to immiscible flow problems with discontinuous permeability or diffusivity. The solutions to the PDEs derived from interface problems are typically discontinuous at the interface, which often causes conventional numerical methods to fail.

With the widespread adoption of small and medium-sized servers and the continuous improvement of computing performance in large supercomputing centers, scientific computing has gradually become the third major research method, alongside theory and experimentation. The Immersed Interface Method [1–3], developed by experts, has been applied to model blood circulation in the human heart. This method integrates mathematical modeling with numerical discretization, enhancing computational efficiency. Several researchers have extended the Immersed Interface Method [4, 5] to address elliptic equations with discontinuous coefficients and singularities in the source terms. For elliptic interface problems, the Harmonic Averaging Method [6, 7] was proposed as an alternative. However, while the Harmonic Averaging Method performs well for one-dimensional elliptic interface problems, it requires significant computational effort when solving high-dimensional problems, and the integral terms involved are methodologically challenging to implement.

In recent years, numerous scholars have continued to explore elliptic interface problems. Bell et al. [7] and Xu et al. [8, 9] proposed finite difference methods for solving boundary value problems. Lin et al. [10] evaluated the errors of various immersed finite element techniques for solving elliptic interface problems, considering both correct and incorrect interface jump conditions. Meanwhile, Wang et al. [11] developed a multiscale discontinuous Galerkin strategy for second-order elliptic problems with heterogeneous coefficients. In the context of hybridizable discontinuous Galerkin methods, Xu et al. in [12] proposed a linear finite element method for a second-order elliptic equation in non-divergence form with Cordes coefficients; Efendiev et al. [13] introduced a novel model reduction approach. Gao et al. [14] proposed a mixed finite volume method for solving second-order elliptic equations with Neumann boundary conditions. In contrast, Feng et al. [15] designed a high-order compact finite difference method for elliptic interface problems with discontinuous and sharply varying coefficients. Finally, Ji et al. [16] offered valuable insights into nonconforming immersed finite element methods that use edge integrals as degrees of freedom to solve elliptic interface problems. Xu et al. [17] and Chen et al. [18] also proposed efficient multigrid methods for solving semilinear interface problems, extending the existing multigrid strategies to handle more complex semilinear and parabolic interface problems effectively.

Although there are many methods for the elliptical interface problem, the accuracy is not always satisfactory. Therefore, this article proposes a new reproducing kernel method based on Legendre polynomials.

The reproducing kernel method [19, 20] is an analytical technique that uses initial conditions to construct a linear operator and derive the original complex model equation by solving simple linear operator equations. Reproducing kernel theory has found widespread applications in signal processing [21,22], wavelet transforms [23], machine learning [24,25], and other fields of research in recent years. It has proven highly effective for solving linear, nonlinear integral, and differential equations [26–28]. For example, Du and Cui used the reproducing kernel method to solve the forced Duffing equation with integral boundary conditions [26]. Xu et al. used this method to solve the one-dimensional elliptic interface problem [28]. Niu et al. used the reproducing kernel method to solve the nonlinear Caputo type q-fractional initial value problem [27]. Additionally, for Eq (1.1), a broken reproducing kernel method has been proposed by [29].

The method presented in this work is exemplified by the following model:

$$\begin{cases} -(\beta_1 u')' + \gamma_1 u' + \delta_1 u = f_1(x), & 0 < x < \alpha_1, \\ -(\beta_2 u')' + \gamma_2 u' + \delta_2 u = f_2(x), & \alpha_1 < x < \alpha_2, \\ -(\beta_3 u')' + \gamma_3 u' + \delta_3 u = f_3(x), & \alpha_2 < x < 1, \\ u(0) = A, \quad u(1) = B, \\ [u]_{\alpha_1} = [u]_{\alpha_2} = 0, \ [\beta u']_{\alpha_1} = [\beta u']_{\alpha_2} = 0, \end{cases} \tag{1.1}$$

The last line of Eq (1.1) expresses the interface conditions satisfied by the solution on the interface, which are presented as follows:

$$\begin{aligned} [u]_{\alpha_i} &= u(\alpha_i^+) - u(\alpha_i^-), \\ [\beta u']_{\alpha_i} &= \beta_{i+1}(\alpha_i^+) u'(\alpha_i^+) - \beta_i(\alpha_i^-) u'(\alpha_i^-), \ i = 1, 2. \end{aligned}$$

The specific requirements for the parameters in Eq (1.1) are detailed in [30]. Unlike [29], this work presents a numerical approach based on reproducing kernel space theory to solve the two-point interface problem. These problems are investigated both theoretically and numerically using the reproducing kernel method in conjunction with Legendre polynomial properties. To validate the algorithm and improve its practical application, the analysis includes proving the existence and uniqueness of the solution, highlighting the method's reliability and efficiency.

The organization of this paper is as follows: Section 2 introduces a new reproducing kernel space constructed with Legendre polynomials. In Section 3, three linear operators are defined, the solution space for Eq (1.1) is established, and the existence and uniqueness of the solution are validated. Section 4 covers the analysis of convergence and the estimation of errors. In section 5, examples are given to validate the algorithm. Finally, the conclusion is drawn.

2. Preliminaries

We first set up the necessary reproducing kernel spaces.

Definition 1. *The reproducing kernel space $W_2^m[a,b]$ is defined by*

$$W_2^m[a,b] = \Big\{ u(t) \mid u^{(m-1)}(t) \text{ is an absolutely continuous real value function in } [a,b], \; u^{(m)}(t) \in L^2[a,b] \Big\}. \tag{2.1}$$

The inner product and norm in $W_2^m[a,b]$ are given as

$$\begin{cases} \langle u, v \rangle_{W_2^m[a,b]} = \sum_{i=0}^{m-1} u^{(i)}(a) v^{(i)}(a) + \int_a^b u^{(m)} v^{(m)} dt, \quad u, v \in W_2^m[a,b], \\ \|u\|_{W_2^m} = \sqrt{\langle u, u \rangle_{W_2^m}}. \end{cases} \tag{2.2}$$

Definition 2. *Let A_n be the Legendre polynomials on the interval $[-1, 1]$. More specifically,*

$$A_0(t) = 1, \ A_1(t) = t, \ A_n(t) = \frac{2n-1}{n} t A_{n-1}(t) - \frac{n-1}{n} A_{n-2}(t), \ n = 2, 3, \cdots.$$

Lemma 1. *Let* $\widehat{A_n}(x) = A_n\left(\frac{2}{b-a}x - \frac{b+a}{b-a}\right)$. *Then we have*

$$\langle \widehat{A_m}, \widehat{A_n} \rangle = \int_a^b \widehat{A_m}(x)\widehat{A_n}(x)dx = \begin{cases} \dfrac{b-a}{2n+1} & m = n, \\ \\ 0 & m \neq n. \end{cases}$$

Lemma 2. *Let*

$$R_t(s) = \sum_{k=0}^{\infty} e_k(s)e_k(t).$$

where

$$e_i = \frac{\widehat{A_i}}{\sqrt{(b-a)/(2i+1)}}, i = 0, 1, 2, \cdots,$$

Then $R_t(s)$ *is the reproducing kernel of* $W_2^m[a,b]$.

Proof. According to Lemma 1, the set $\{e_i\}_{i=0}^{\infty}$ constitutes a standard orthogonal basis of $W_2^m[a,b]$. Furthermore,

$$\langle R_t(s), f(s) \rangle = \langle \sum_{k=0}^{\infty} e_k(s)e_k(t), f(s) \rangle = \sum_{k=0}^{\infty} \langle e_k(s), f(s) \rangle e_k(t) = f(t),$$

which proves that $R_t(s)$ is a reproducing kernel of $W_2^m[a,b]$. □

Owing to the interface, the continuity of the derivative in Eq (1.1) is disrupted, making the conventional reproducing kernel space $W_2^m[0,1]$ unsuitable for interface problems. Consequently, we establish a new reproducing kernel space $H_2^m[0,1]$ tailored for these issues.

Lemma 3. *[29]*

$$H_2^m[0,1] = \left\{ u(x) \mid u(x) = \begin{cases} u_1(x), & 0 \le x \le \alpha_1, \quad u_1(x) \in W_2^m[0,\alpha_1] \\ u_2(x), & \alpha_1 < x \le \alpha_2, \ u_2(x) \in W_2^m[\alpha_1,\alpha_2] \\ u_3(x), & \alpha_2 < x \le 1, \quad u_3(x) \in W_2^m[\alpha_2,1] \end{cases} \right\}$$

is a reproducing kernel space. For any $u, v \in H_2^m[0,1]$, *the inner product and norm are as follows:*

$$\begin{cases} \langle u, v \rangle_{H_2^m[0,1]} = \langle u_1, v_1 \rangle_{W_2^m[0,\alpha_1]} + \langle u_2, v_2 \rangle_{W_2^m[\alpha_1,\alpha_2]} + \langle u_3, v_3 \rangle_{W_2^m[\alpha_2,1]}, \\ \\ \|u\|_{H_2^m[0,1]} = (\|u_1\|^2_{W_2^m[0,\alpha_1]} + \|u_2\|^2_{W_2^m[\alpha_1,\alpha_2]} + \|u_3\|^2_{W_2^m[\alpha_2,1]})^{\frac{1}{2}} \end{cases}$$

Let $r_y^m(x)$ be the reproducing kernel of $W_2^m[0,\alpha_1]$, the same as $s_y^m(x)$ and $t_y^m(x)$, we can get the following reproducing kernel function of $H_2^m[0,1]$.

$$R_y^m(x) = \begin{cases} r_y^m(x), & 0 \le x, y \le \alpha_1, \\ s_y^m(x), & \alpha_1 < x, y \le \alpha_2, \\ t_y^m(x), & \alpha_2 < x, y \le 1, \\ 0, & \text{others}. \end{cases} \tag{2.3}$$

3. Reproducing kernel method

Define three linear operators.

$$\begin{aligned}
&\mathcal{D}_1 : W_2^m[0,\alpha_1] \to W_2^{m-2}[0,\alpha_1],\\
&\mathcal{D}_2 : W_2^m[\alpha_1,\alpha_2] \to W_2^{m-2}[\alpha_1,\alpha_2],\\
&\mathcal{D}_3 : W_2^m[\alpha_2,1] \to W_2^{m-2}[\alpha_2,1].
\end{aligned}$$

Let

$$\mathcal{D}(u) = \begin{cases} \mathcal{D}_1(u) = -(\beta_1 u')' + \gamma_1 u' + \delta_1 u, & 0 \le x < \alpha_1,\\ \mathcal{D}_2(u) = -(\beta_2 u')' + \gamma_2 u' + \delta_2 u, & \alpha_1 \le x < \alpha_2,\\ \mathcal{D}_3(u) = -(\beta_3 u')' + \gamma_3 u' + \delta_3 u, & \alpha_2 \le x \le 1 \end{cases} \tag{3.1}$$

be a linear bounded operator. $M_1 = \{x_{1,i}\}_{i=1}^{N_1}$, $M_2 = \{x_{2,i}\}_{i=1}^{N_2}$, and $M_3 = \{x_{3,i}\}_{i=1}^{N_3}$. Write the conjugate operator of $\mathcal{D}_y$ as $\mathcal{D}_y^*$. Let

$$\begin{aligned}
\psi_i^m(x) &= \mathcal{D}_y^* R_y^{m-2}(x)|_{y=x_{1,i}}, i = 1,2\cdots N_1\\
\phi_i^m(x) &= \mathcal{D}_y^* R_y^{m-2}(x)|_{y=x_{2,i}}, i = 1,2\cdots N_2\\
\Phi_i^m(x) &= \mathcal{D}_y^* R_y^{m-2}(x)|_{y=x_{3,i}}, i = 1,2\cdots N_3
\end{aligned}$$

Because of properties of the conjugate operator, we can obtain

$$\begin{aligned}
\psi_i^m(x) &= \mathcal{D}_y R_y^m(x)\Big|_{y=x_{1,i}},\\
\phi_i^m(x) &= \mathcal{D}_y R_y^m(x)\Big|_{y=x_{2,i}},\\
\Phi_i^m(x) &= \mathcal{D}_y R_y^m(x)\Big|_{y=x_{3,i}}.
\end{aligned} \tag{3.2}$$

Considering the interface conditions and boundary conditions, we define

$$\begin{aligned}
\varphi_1^m(x) &= R_y^m(x)|_{y=0},\\
\varphi_2^m(x) &= R_y^m(x)|_{y=1},\\
\varphi_3^m(x) &= \begin{cases} -r_y^m(x)|_{y=\alpha_1}, & 0 \le x \le \alpha_1,\\ s_y^m(x)|_{y=\alpha_1}, & \alpha_1 < x \le \alpha_2,\\ 0, & \alpha_2 < x \le 1, \end{cases}\\
\varphi_4^m(x) &= \begin{cases} -\beta_1(\alpha_1^-)\dfrac{\partial r_y^m(x)}{\partial y}|_{y=\alpha_1}, & 0 \le x \le \alpha_1,\\ \beta_2(\alpha_1^+)\dfrac{\partial s_y^m(x)}{\partial y}|_{y=\alpha_1}, & \alpha_1 < x \le \alpha_2,\\ 0, & \alpha_2 < x \le 1, \end{cases}\\
\varphi_5^m(x) &= \begin{cases} 0, & 0 \le x \le \alpha_1,\\ -s_y^m(x)|_{y=\alpha_2}, & \alpha_1 < x \le \alpha_2,\\ t_y^m(x)|_{y=\alpha_2}, & \alpha_2 < x \le 1, \end{cases}
\end{aligned}$$

$$\varphi_6^m(x)=\begin{cases}0, & 0\le x\le\alpha_1,\\ -\beta_2(\alpha_2^-)\dfrac{\partial s_y^m(x)}{\partial y}|_{y=\alpha_2}, & \alpha_1<x\le\alpha_2,\\ \beta_3(\alpha_2^+)\dfrac{\partial t_y^m(x)}{\partial y}|_{y=\alpha_2}, & \alpha_2<x\le 1.\end{cases}$$

Lemma 4. *In fact,* $\{\psi_1^m,\psi_2^m,\cdots,\psi_{N_1}^m,\phi_1^m,\phi_2^m,\cdots,\phi_{N_2}^m,\Phi_1^m,\Phi_2^m,\cdots,\Phi_{N_3}^m,\varphi_1^m,\ \varphi_2^m,\cdots\varphi_6^m\}$ *is linearly independent.*

Let $n=N_1+N_2+N_3+6$, then we define the approximating solution space U_n^m as follows:

$$U_n^m=\text{span}\{\psi_1^m,\psi_2^m,\cdots,\psi_{N_1}^m,\phi_1^m,\phi_2^m,\cdots,\phi_{N_2}^m,\Phi_1^m,\Phi_2^m,\cdots,\Phi_{N_3}^m,\varphi_1^m,\varphi_2^m,\cdots\varphi_6^m\}.$$

Therefore, we find the solution of Eq (1.1), which is equivalent to, finding $u_n^m(x)\in U_n^m$ such that

$$u_n^m(x)=\sum_{i=1}^{N_1}\lambda_i^m\psi_i^m(x)+\sum_{j=1}^{N_2}\mu_j^m\phi_j^m(x)+\sum_{k=1}^{N_3}\sigma_k^m\Phi_k^m(x)+\sum_{l=1}^{6}\delta_l^m\varphi_l^m(x), \tag{3.3}$$

where $\lambda_1^m,\lambda_2^m,\cdots,\lambda_{N_1}^m,\mu_1^m,\mu_2^m,\cdots,\mu_{N_2}^m,\sigma_1^m,\sigma_2^m,\cdots,\sigma_{N_3}^m,\delta_l^m,\delta_2^m,\cdots,\delta_6^m$ are undetermined coefficients. We apply the numerical method for Eq (1.1) at the above $N_1+N_2+N_3$ different points, providing that

$$\begin{aligned}\mathcal{D}_1u_n^m(\lambda_i^m)&=f_1(\lambda_i^m),\ i=1,\ 2,\ \cdots,N_1,\\ \mathcal{D}_2u_n^m(\mu_j^m)&=f_2(\mu_j^m),\ j=1,\ 2,\ \cdots,\ N_2,\\ \mathcal{D}_3u_n^m(\sigma_k^m)&=f_3(\sigma_k^m),\ k=1,\ 2,\ \cdots,\ N_3.\end{aligned} \tag{3.4}$$

The other additional equations satisfy the following constraints:

$$u_n^m(0)=A,\quad u_n^m(1)=B, \tag{3.5}$$

$$[u_n^m]_{\alpha_1}=[u_n^m]_{\alpha_2}=0,\ \ [\beta(u_n^m)']_{\alpha_1}=[\beta(u_n^m)']_{\alpha_2}=0. \tag{3.6}$$

We get the matrix form equation

$$G_mx_m=H, \tag{3.7}$$

where

$$G_m=\begin{pmatrix}\langle\psi_i^m,\psi_i^m\rangle_{N_1\times N_1} & \langle\psi_i^m,\phi_j^m\rangle_{N_1\times N_2} & \langle\psi_i^m,\Phi_k^m\rangle_{N_1\times N_3} & \langle\psi_i^m,\varphi_l^m\rangle_{N_1\times 6}\\ \langle\phi_j^m,\psi_i^m\rangle_{N_2\times N_1} & \langle\phi_j^m,\phi_j^m\rangle_{N_2\times N_2} & \langle\phi_j^m,\Phi_k^m\rangle_{N_2\times N_3} & \langle\phi_j^m,\varphi_l^m\rangle_{N_2\times 6}\\ \langle\Phi_k^m,\psi_i^m\rangle_{N_3\times N_1} & \langle\Phi_k^m,\phi_j^m\rangle_{N_3\times N_2} & \langle\Phi_k^m,\Phi_k^m\rangle_{N_3\times N_3} & \langle\Phi_j^m,\varphi_l^m\rangle_{N_3\times 6}\\ \langle\varphi_l^m,\psi_i^m\rangle_{6\times N_1} & \langle\varphi_l^m,\phi_j^m\rangle_{6\times N_2} & \langle\varphi_l^m,\Phi_k^m\rangle_{6\times N_3} & \langle\varphi_l^m,\varphi_l^m\rangle_{6\times 6}\end{pmatrix} \tag{3.8}$$

$$x_m=(\lambda_1^m,\ \lambda_2^m,\ \cdots,\ \lambda_{N_1}^m,\ \mu_1^m,\ \mu_2^m,\ \cdots,\ \mu_{N_2}^m,\ \sigma_1^m,\ \sigma_2^m,\ \cdots,\ \sigma_{N_3}^m,\ \delta_1^m,\ \delta_2^m,\ \cdots,\ \delta_6^m)^T,$$
$$H=(f(x_1^1),\ \cdots,\ f(x_{N_1}^1),\ f(x_1^2),\ \cdots,\ f(x_{N_2}^2),\ f(x_1^3),\ \cdots,\ f(x_{N_3}^3),\ A,\ B,\ 0,\ 0,\ 0,\ 0)^T.$$

Finding the solutions x_m of the matrix equation (3.7), then the approximating solution

$$u_n^m(x)=\mathcal{P}_n^mu=\sum_{i=1}^{N_1}\lambda_i^m\psi_i^m(x)+\sum_{j=1}^{N_2}\mu_j^m\phi_j^m(x)+\sum_{k=1}^{N_3}\sigma_k^m\Phi_k^m(x)+\sum_{l=1}^{6}\delta_l^m\varphi_l^m(x)\in U_n^m$$

is obtained, where $\mathcal{P}_n^m: H_2^m[0,1]\to U_n^m$ is the orthogonal projection operator.

Lemma 5. *Eqs* (3.4)–(3.6) *have a unique solution.*

Proof. It is easy to verify

$$\begin{aligned}
\mathcal{D}_1u_n^m(\lambda_i^m) &= \langle u_n^m, \psi_i^m\rangle_{H_2^m[0,1]}, \quad i=1,2,\ldots,N_1,\\
\mathcal{D}_2u_n^m(\mu_j^m) &= \langle u_n^m, \phi_j^m\rangle_{H_2^m[0,1]}, \quad j=1,2,\ldots,N_2,\\
\mathcal{D}_3u_n^m(\sigma_k^m) &= \langle u_n^m, \Phi_k^m\rangle_{H_2^m[0,1]}, \quad k=1,2,\ldots,N_3,\\
u_n^m(0) &= \langle u_n^m, \varphi_1^m\rangle_{H_2^m[0,1]},\\
u_n^m(1) &= \langle u_n^m, \varphi_2^m\rangle_{H_2^m[0,1]},\\
[u_n^m]_{\alpha_1} &= \langle u_n^m, \varphi_3^m\rangle_{H_2^m[0,1]},\\
[\beta(u_n^m)']_{\alpha_1} &= \langle u_n^m, \varphi_4^m\rangle_{H_2^m[0,1]},\\
[u_n^m]_{\alpha_2} &= \langle u_n^m, \varphi_5^m\rangle_{H_2^m[0,1]},\\
[\beta(u_n^m)']_{\alpha_2} &= \langle u_n^m, \varphi_6^m\rangle_{H_2^m[0,1]}.
\end{aligned}$$

Therefore, the coefficient matrix in Eq (3.4)–(3.6) is positive definite and symmetric, which confirms that these equations possess a single unique solution.

□

4. Convergence and error analysis

Theorem 1. *Given that u_n^m serves as an approximate solution to the Eq (1.1), it will converge uniformly to the true solution u over the interval* $[0,1]$.

Proof. By the properties of the projection operator, it is known that as $n\to\infty$, $\|u-\mathcal{D}u\|_{H_2^m[0,1]}\to 0$. Moreover,

$$\begin{aligned}
|u_n^m(x)-u(x)| &= \left|\langle u_n^m(\cdot)-u(\cdot), R_x^m(\cdot)\rangle\right|_{H_2^m[0,1]}\\
&\le \|u_n^m-u\|_{H_2^m[0,1]}\left(\|r_x^m\|_{W_2^m[0,\alpha_1]}+\|s_x^m\|_{W_2^m[\alpha_1,\alpha_2]}+\|t_x^m\|_{W_2^m[\alpha_2,1]}\right)
\end{aligned}$$

Given that $\|r_x^m\|_{W_2^m[0,\alpha_1]}$, $\|s_x^m\|_{W_2^m[\alpha_1,\alpha_2]}$, and $\|t_x^m\|_{W_2^m[\alpha_2,1]}$ are restricted within bounds, the sum $\|r_x^m\|_{W_2^m[0,\alpha_1]}+\|s_x^m\|_{W_2^m[\alpha_1,\alpha_2]}+\|t_x^m\|_{W_2^m[\alpha_2,1]}$ is less than or equal to some positive real number M. Therefore, u_n^m uniformly converges to u on the interval $[0,1]$. □

Theorem 2. *Suppose $u\in H_2^3$ is the solution of the system of Eqs* (1.1)*, and u_n^m is the solution of the system of Eqs* (3.4)–(3.6) *in the space U_n^3. Then we have*

$$\|u-u_n^m\|_{H_2^3[0,1]}\le C_1 d\|u\|_{H_2^3[0,1]}. \tag{4.1}$$

and

$$\|u-u_n^m\|_{L^\infty}\le C_2 d^2\|u\|_{H_2^3[0,1]}, \tag{4.2}$$

where

$$d=\max_{2\le i\le N_1, 2\le j\le N_2, 2\le k\le N_3}\{x_i-x_{i-1}, x_j-x_{j-1}, x_k-x_{k-1}\},$$

and C_1, C_2, and C_3 are constants independent of d.

Proof. Assuming $u \in H_2^3$ and $f \in H_2^1[0,1]$. Here, we take $m = 3$, and then the representations of u can be expressed by the following:

$$u(x) = \begin{cases} u_1(x), & 0 \leq x \leq \alpha_1, \\ u_2(x), & \alpha_1 < x \leq \alpha_2, , \\ u_3(x), & \alpha_2 < x \leq 1, \end{cases}$$

and the approximating solution u_n^m can be correspondingly expressed by:

$$u_n^m(x) = \begin{cases} u_{1,n}^m(x), & 0 \leq x \leq \alpha_1, \\ u_{2,n}^m(x), & \alpha_1 < x \leq \alpha_2, \\ u_{3,n}^m(x), & \alpha_2 < x \leq 1, \end{cases}$$

Let $V_{N_1} = \text{span}\{(\mathcal{D}_1)_y r_y^3|_{y=x_i}^{N_1}\}$, $V_{N_2} = \text{span}\{(\mathcal{D}_2)_y s_y^3|_{y=x_i}^{N_2}\}$, $V_{N_3} = \text{span}\{(\mathcal{D}_3)_y t_y^3|_{y=x_i}^{N_3}\}$, where Q_{N_1}, Q_{N_2} and Q_{N_3} are the orthogonal projection operators from $W_2^3[0,\alpha_1]$, $W_2^3[\alpha_1,\alpha_2]$, and $W_2^3[\alpha_2,1]$ to V_{N_1}, V_{N_2} and V_{N_3}, respectively. First, we prove $u_{1,n}^m = Q_{N_1}u_1$, $u_{2,n}^m = Q_{N_2}u_2$ and $u_{3,n}^m = Q_{N_3}u_3$. Then, from the existing results [31], we estimate $\|u_1 - Q_{N_1}u_1\|_{W_2^3[0,\alpha_1]}$, $\|u_2 - Q_{N_2}u_2\|_{W_2^3[\alpha_1,\alpha_2]}$ and $\|u_3 - Q_{N_3}u_3\|_{W_2^3[\alpha_2,1]}$. Finally, by the norm $\|\cdot\|_{H_2^3[0,1]}$ and the definition of the projection operator, we can estimate Eqs (4.1) and (4.2). We know that for $1 \leq i \leq N_1$,

$$\begin{aligned} \langle Q_{N_1}u_1, \mathcal{D}_1 r_{x_i}^3\rangle_{W_2^3[0,\alpha_1]} &= \langle u_1, \mathcal{D}_1 r_{x_i}^3\rangle_{W_2^3[0,\alpha_1]} = \langle u, \psi_i^3\rangle_{H_2^3[0,1]}, \\ &= \langle u_n^m, \psi_i^3\rangle_{H_2^3[0,1]} = \langle u_{n_1}^m, \mathcal{D}_1 r_{x_i}^3\rangle_{W_2^3[0,\alpha_1]}. \end{aligned}$$

This indicates that $u_{1,n}^m = Q_{N_1}u_1$, similarly, $u_{2,n} = Q_{N_2}u_2$, and $u_{3,n} = Q_{N_3}u_3$. Next, from the existing results [31], we know that the following inequalities hold:

$$\|u_1 - Q_{N_1}u_1\|_{W_2^3[0,\alpha_1]} \leq c_1 d\|u_1\|_{W_2^3[0,\alpha_1]} \leq c_2 d\|u_1\|_{W_2^1[0,\alpha_1]}, \tag{4.3}$$

$$\|u_2 - Q_{N_2}u_2\|_{W_2^3[\alpha_1,\alpha_2]} \leq c_3 d\|u_2\|_{W_2^3[\alpha_1,\alpha_2]} \leq c_4 d\|u_2\|_{W_2^1[\alpha_1,\alpha_2]}, \tag{4.4}$$

$$\|u_3 - Q_{N_3}u_3\|_{W_2^3[\alpha_2,1]} \leq c_5 d\|u_3\|_{W_2^3[\alpha_2,1]} \leq c_6 d\|u_3\|_{W_2^1[\alpha_2,1]}, \tag{4.5}$$

In this case, c_1, c_2, c_3, c_4, c_5, and c_6 represent positive constants independent of d. Based on the norm $|\cdot|_{H_2^3[0,1]}$ as defined, it follows that:

$$\|u - u_n^m\|_{H_2^3[0,1]}^2 = \|u_1 - u_{1,n}^m\|_{W_2^3[0,\alpha_1]}^2 + \|u_2 - u_{2,n}^m\|_{W_2^3[\alpha_1,\alpha_2]}^2 + \|u_3 - u_{3,n}^m\|_{W_2^3[\alpha_2,1]}^2.$$

Therefore, the estimation in (4.1) can be deduced from (4.3)-(4.5). Similarly, we can obtain the following estimate :

$$\|R_x^3 - \mathcal{P}_n R_x^3\|_{H_2^3[0,1]} \leq c_8 d\|R_x\|_{H_2^1[0,1]},$$

Here, c_7 and c_8 are independent of d and represent positive constants. In conclusion, by utilizing the properties of the projection operator along with the Cauchy-Schwarz inequality, we can obtain

$$\begin{aligned} |u(x) - u_n^m(x)| &= \langle u(\cdot) - u_n^m(\cdot), R_x^3(\cdot)\rangle_{H_2^3[0,1]} \\ &= \langle u(\cdot) - u_n^m(\cdot), R_x^3(\cdot) - \mathcal{P}_n R_x^3(\cdot)\rangle_{H_2^3[0,1]} \\ &\leq \|u - u_n^m\|_{H_2^3[0,1]}\|R_x^3 - \mathcal{P}_n R_x^3\|_{H_2^3[0,1]} \\ &\leq C_1 d^2\|u\|_{H_1^2[0,1]}, \end{aligned}$$

where C_1 is constant independent of d. The estimation in (4.2) can be derived accordingly. □

5. Numerical examples

In this section, we provide some numerical examples to test our presented method. For the sake of convenience, we use the following notations to represent various types of errors.

$$\|e\|_\infty = \max_{0<x<1}|u-u_n^3|, \|e\|_0 = \left(\int_0^1 \left(u-u_n^3\right)^2 \,\mathrm{d}x\right)^{1/2},$$

$$\|e\|_1 = \left(\int_0^{\alpha_1} \left(u'-u_n^{3\prime}\right)^2 \,\mathrm{d}x + \int_{\alpha_1}^{\alpha_2} \left(u'-u_n^{3\prime}\right)^2 \,\mathrm{d}x + \int_{\alpha_2}^{1} \left(u'-u_n^{3\prime}\right)^2 \,\mathrm{d}x\right)^{1/2},$$

$$\|e\|_2 = \left(\int_0^{\alpha_1} \left(u''-u_n^{3\prime\prime}\right)^2 \,\mathrm{d}x + \int_{\alpha_1}^{\alpha_2} \left(u''-u_n^{3\prime\prime}\right)^2 \,\mathrm{d}x + \int_{\alpha_2}^{1} \left(u''-u_n^{3\prime\prime}\right)^2 \,\mathrm{d}x\right)^{1/2}.$$

Example 1. *Take into account the system of equations [29, 30].*

$$\begin{cases} -(u')' = f_1(x), & 0 \le x < 0.4, \\ -(10^{-3}u')' = f_2(x), & 0.4 < x < 0.7, \\ -(10u')' = f_3(x), & 0.7 < x \le 1, \\ [u]_{0.4} = [u]_{0.7} = 0, \;\; [\beta u']_{0.4} = [\beta u']_{0.7} = 0. \end{cases} \tag{5.1}$$

where the functions $f_i(x)(i = 1, 2, 3)$ *are determined by the following exact solution:*

$$u(x) = \begin{cases} -\frac{x^2}{2}, & x \in [0, 0.4), \\ -\frac{1}{10^{-3}}\frac{x^2}{2} - \left(1-\frac{1}{10^{-3}}\right)\frac{2}{25}, & x \in (0.4, 0.7], \\ \frac{1}{10}f(x) - \left(1-\frac{1}{10^{-3}}\right)\frac{2}{25} - \left(\frac{1}{10^{-3}}-\frac{1}{10}\right)\frac{49}{200}, & x \in (0.7, 1]. \end{cases} \tag{5.2}$$

Table 1 presents a comparison between our methods [29], the exact solution, and the approximation. Table 2 details the absolute errors across various norms. Furthermore, Table 3 evaluates our approach against several existing methods. Figure 1 highlights the solution comparisons, whereas Figure 2 illustrates the absolute errors associated with $u(x)$ *and* $u'(x)$*. Our comparisons reveal that our approach demonstrates higher accuracy.*

Table 1. Absolute error and the numerical result for Example 1.

	BRKM [29]			Our Method		
Code	$u(x)$	$u_n(x)$	$\lvert u_n(x)-u(x)\rvert$	$u(x)$	$u_n(x)$	$\lvert u_n(x)-u(x)\rvert$
0.1	-0.005	-0.005	7.61046e-7	-0.005	-0.005	4.90e-10
0.2	-0.02	-0.02	1.43987e-6	-0.02	-0.02	8.15e-10
0.3	-0.045	-0.045	1.85999e-6	-0.045	-0.045	1.19e-9
0.4	-0.08	-0.08	2.0474e-6	-0.08	-0.08	1.53e-9
0.5	-170.08	-170.08	7.99284e-5	-170.08	-170.08	1.15e-9
0.6	-280.08	-280.08	2.8774e-5	-280.08	-280.08	6.20e-10
0.7	-410.08	-410.08	7.81988e-5	-410.08	-410.08	6.93e-11
0.8	569.839	569.839	4.11343e-5	569.839	569.839	1.08e-11
0.9	569.83	569.83	2.53934e-5	569.83	569.83	9.45e-11

Table 2. The error in different type norms for Example 1.

N_1	N_2	N_3	$\|\|e\|\|_\infty$	$\|\|e\|\|_0$	$\|\|e\|\|_1$	$\|\|e\|\|_2$
4	2	2	5.46e-12	5.60e-11	2.79e-10	3.58e-9
5	3	3	5.56e-11	3.24e-11	1.32e-9	4.78e-8
8	3	5	1.33e-10	8.18e-10	4.68e-9	2.41e-7

Table 3. Comparison of the maximum errors of different methods for Example 1.

n	BRKM [29]	HA [30]	AA [30]	Our Method
12	1.90e-4	5.79e-2	2.89e-1	2.68e-10
22	4.27e-7	1.48e-2	1.62e-1	1.97e-9

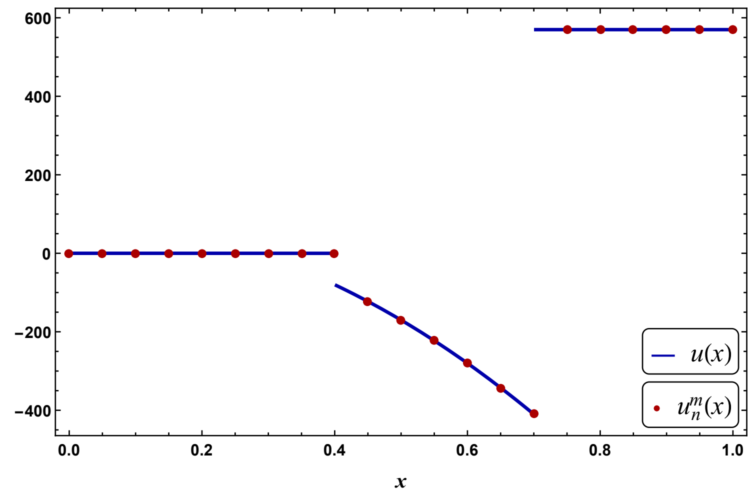

Figure 1. Numerical result with $N_1 = 8,\ N_2 = 3,\ N_3 = 5$ for Example 1.

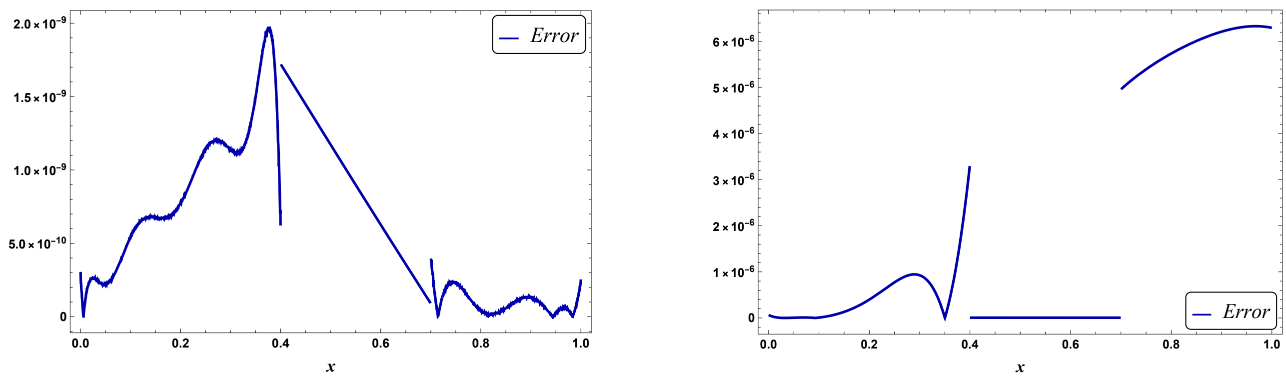

Figure 2. $|u_n(x) - u(x)|$(Left) and $|u_n'(x) - u'(x)|$(Right) with $N_1 = 8,\ N_2 = 3,\ N_3 = 5$ for Example 1.

Example 2. *Take the following set of equations into account [29].*

$$\begin{cases} -(u')' = f_1(x), & 0 < x < \dfrac{1}{2}, \\ -(2u')' = f_2(x), & \dfrac{1}{2} < x < \dfrac{1}{2} + 0.05, \\ -(80u')' = f_3(x), & \dfrac{1}{2} + 0.05 < x < 1, \\ [u]_{\frac{1}{2}} = [u]_{\frac{1}{2}+0.05} = 0, \ [\beta u']_{\frac{1}{2}} = [\beta u']_{\frac{1}{2}+0.05} = 0. \end{cases} \tag{5.3}$$

where the functions $f_i(x)(i = 1, 2, 3)$ are determined by the following exact solution:

$$u(x) = \begin{cases} x^4, & x \in \left[0, \dfrac{1}{2}\right), \\ \frac{1}{2}x^4 + \frac{1}{32}, & x \in \left(\dfrac{1}{2}, \dfrac{1}{2} + 0.05\right], \\ \frac{1}{80}x^4 + \frac{1}{32} + \frac{39}{80}\left(\frac{1}{2} + 0.05\right)^4, & x \in \left(\dfrac{1}{2} + 0.05, 1\right]. \end{cases} \tag{5.4}$$

The exact, approximate, and absolute solutions, along with their corresponding errors, are presented in Table 4 and compared with the techniques described in [29]. Table 5 shows the errors in different types of norms. The solution comparison is illustrated in Figure 3. Figure 4 shows the absolute error of $u(x)$.

Table 4. Absolute error and the numerical result for Example 2.

	BRKM [29]			Our Method		
Code	$u(x)$	$u_n(x)$	$\|u_n(x) - u(x)\|$	$u(x)$	$u_n(x)$	$\|u_n(x) - u(x)\|$
0.1	0.0001	0.0000194472	8.05528e-5	0.0001	0.000100107	1.07e-7
0.2	0.0016	0.00146845	1.31553e-4	0.0016	0.00160021	2.13e-7
0.3	0.0081	0.00796198	1.3802e-4	0.0081	0.00810032	3.20e-7
0.4	0.0256	0.0255	9.99946e-5	0.0256	0.0256004	4.27e-7
0.5	0.0625	0.0624673	3.27147e-5	0.0625	0.0625005	5.34e-7
0.6	0.0774793	0.0774676	1.17187e-5	0.0774793	0.0774794	1.51e-7
0.7	0.0788605	0.0788503	1.02034e-5	0.0788605	0.0788607	1.13e-7
0.8	0.0809793	0.0809716	7.6943e-6	0.0809793	0.0809794	7.55e-8
0.9	0.0840605	0.0840564	4.15465e-6	0.0840605	0.0840606	3.77e-8

Table 5. The error in different type norms for Example 2.

N_1	N_2	N_3	$\|\|e\|\|_\infty$	$\|\|e\|\|_0$	$\|\|e\|\|_1$	$\|\|e\|\|_2$
5	3	3	6.36e-5	3.57e-5	1.45e-4	1.60e-3
8	3	5	8.56e-8	2.39e-7	2.18e-6	2.60e-4
16	6	10	7.33e-12	9.91e-12	6.28e-11	2.05e-8

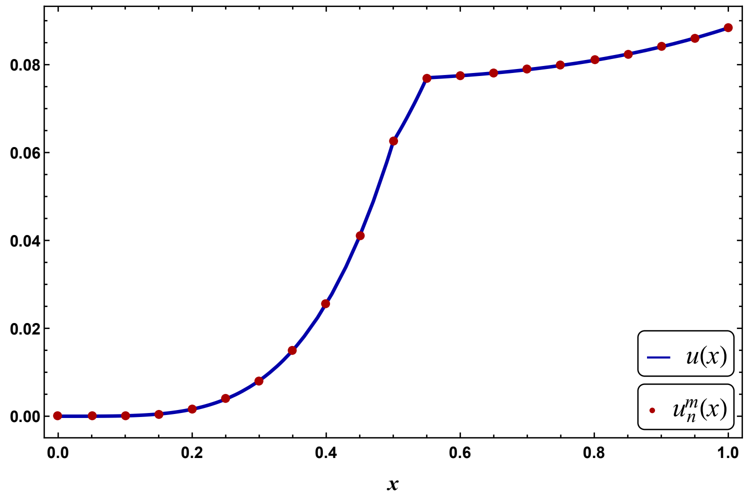

Figure 3. Numerical result with $N_1 = 8, \ N_2 = 3, \ N_3 = 5$ for Example 2.

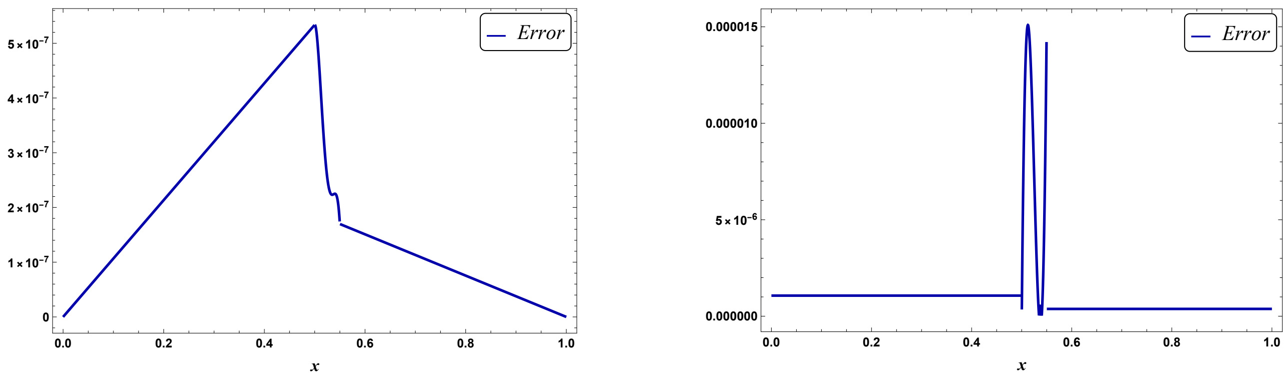

Figure 4. $|u_n(x) - u(x)|$(Left) and $|u_n'(x) - u'(x)|$(Right) with $N_1 = 8, \ N_2 = 3, \ N_3 = 5$ for Example 2.

6. Conclusions

This paper introduces an effective numerical algorithm using reproducing kernel functions and Legendre polynomials to address multiple interface problems. We developed a set of new bases in the reproducing kernel space and transformed model equations into matrix equations. By solving these matrix equations, we obtained approximate solutions. The proposed method outperforms conventional techniques in accuracy. Additionally, the solution's existence and uniqueness are established, highlighting the robustness and practical value of the algorithm.

Author contributions

Min Wu: Conceptualization, Methodology, Software, Writing (Original Draft Preparation). Jiali Zhou: Formal Analysis, Validation, Writing (Review and Editing). Chaoyue Guan: Data Curation, Writing (Review and Editing). Jing Niu : Supervision, Funding Acquisition, Project Administration, Writing (Review and Editing). All authors have read and agreed to the published version of the manuscript.

Use of Generative-AI tools declaration

The authors confirm that no generative AI tools were used in the writing, editing, or data analysis of this manuscript, except for language refinement and grammar checking. All intellectual contributions, including conceptualization, methodology, and validation, were conducted by the authors.

Acknowledgments

This study was supported by the Natural and Science Funds of Heilongjiang Province of China Grant No.LH2024A018. Explore and practice the integrated postgraduate training system of knowledge, action, research, and application Grant No.XJGYJSZ202402. Additionally, it receives support from the "Pioneer" and "Leading Goose" R&D Program of Zhejiang Province, with Grant Numbers 2022C01193, 2022C01178, 2023C01125, 2022C01118, 2023C01130, 2024C01147, 2024C093 and 2024C01059.

Conflict of interest

Authors do not have any conflicts of interest.

References

1. C. S. Peskin, Numerical analysis of blood flow in the heart, *J. Comput. Phys.*, **25** (1977), 220–252. https://doi.org/10.1016/0021-9991(77)90100-0
2. M. F. McCracken, C. S. Peskin, A vortex method for blood flow through heart valves, *J. Comput. Phys.*, **35** (1980), 183–205. https://doi.org/10.1016/0021-9991(80)90085-6
3. P. R. Kramer, C. S. Peskin, Incorporating thermal fluctuations into the immersed boundary method, *Comput. Fluid Solid Mech.*, **47** (2003), 1755–1758. https://doi.org/10.1016/B978-008044046-0.50428-0
4. R. J. LeVeque, Z. L. Li, The immersed interface method for elliptic equations with discontinuous coefficients and singular sources, *SIAM J. Numer. Anal.*, **31** (1994), 1019–1044. https://doi.org/10.1137/0731054
5. S. Z. Deng, K. Ito, Z. L. Li, Three-dimensional elliptic solvers for interface problems and applications, *J. Comput. Phys.*, **184** (2003), 215–243. https://doi.org/10.1016/S0021-9991(02)00028-1
6. A. A. Samarskii, I. V. Fryazinov, On the convergence of a locally one-dimensional scheme for solving the multidimensional equation of heat conduction on non-uniform meshes, *Comput. Math. Math. Phys.*, **11** (1971), 125–144. https://doi.org/10.1016/0041-5553(71)90134-0
7. J. B. Bell, G. R. Shubin, An adaptive grid finite difference method for conservation laws, *J. Comput. Phys.*, **52** (1983), 569–591. https://doi.org/10.1016/0021-9991(83)90008-6

8. M. Xu, R. Lin, L. Zhang, Analysis of the MAC scheme for the three dimensional Stokes problem, *Appl. Numer. Math.*, **19** (2023), 131–147. https://doi.org/10.1016/j.apnum.2023.07.021
9. M. Xu, Ch. Shi, A Hessian recovery-based finite difference method for biharmonic problems, *Appl. Math. Lett.*, **137** (2023), 108503. https://doi.org/10.1016/j.aml.2022.108503
10. T. Lin, Y. Lin, W. Sun, Error estimation of a class of quadratic immersed finite element methods for elliptic interface problems, *Discrete Contin. Dyn. Syst. Ser. B*, **7** (2007), 807. https://doi.org/10.3934/dcdsb.2007.7.807
11. W. Wang, J. Guzman, C. W. Shu, The multiscale discontinuous Galerkin method for solving a class of second order elliptic problems with rough coefficients, *Int. J. Numer. Anal. Model.*, **8** (2011), 28–47.
12. M. Xu, R. Lin, Q. Zou, A C0 linear finite element method for a second-order elliptic equation in non-divergence form with Cordes coefficients, *Numer. Meth. Part. D. E.*, **39** (2023), 2244–2269. https://doi.org/10.1002/num.22965
13. Y. Efendiev, R. Lazarov, M. Moon, K. Shi, A spectral multiscale hybridizable discontinuous Galerkin method for second order elliptic problems, *Comput. Methods Appl. Mech. Eng.*, **292** (2015), 243–256. https://doi.org/10.1016/j.cma.2014.09.036
14. Y. Gao, J. Lv, L. Zhang, Mixed finite volume method for elliptic problems on non-matching multi-block triangular grids, *Int. J. Numer. Anal. Model.*, **14** (2017), 456–476.
15. Q. Feng, B. Han, P. Minev, A high order compact finite difference scheme for elliptic interface problems with discontinuous and high-contrast coefficients, *Appl. Math. Comput.*, **431** (2022), 127314. https://arxiv.org/abs/2105.04600
16. H. Ji, F. Wang, J. Chen, Z. Li, Analysis of nonconforming IFE methods and a new scheme for elliptic interface problems, *ESAIM: Math. Model. Numer. Anal.*, **57** (2023), 2041–2076. https://doi.org/10.1051/m2an/2023047
17. F. Xu, Y. Guo, Q. Huang, H. Ma, An efficient multigrid method for semilinear interface problems, *Appl. Numer. Math.*, **179** (2022), 238–254. https://doi.org/10.1016/j.apnum.2022.05.003
18. F. Chen, M. Cui, C. Zhou, A type of efficient multigrid method for semilinear parabolic interface problems, *Commun. Nonlinear Sci. Numer. Simul.*, **143** (2025), 108632. https://doi.org/10.1016/j.cnsns.2025.108632
19. H. Du, Z. Chen, A new reproducing kernel method with higher convergence order for solving a Volterra-Fredholm integral equation, *Appl. Math. Lett.*, **102** (2020), 106117–106129. https://doi.org/10.1016/j.aml.2019.106117
20. F. Z. Geng, X. Xu, Reproducing kernel functions based univariate spline interpolation, *Appl. Math. Lett.*, **122** (2021), 107525. https://doi.org/10.1016/j.aml.2021.107525
21. J. Romero, E. I. Plotkin, M. N. Swamy, Reproducing kernels and the use of root loci of specific functions in the recovery of signals from non-uniform samples, *Signal Process.*, **49** (1996), 11–23. https://doi.org/10.1016/0165-1684(95)00142-5
22. J. Xian, S. P. Luo, W. Lin, Weighted sampling and signal reconstruction in spline subspaces, *Signal Process.*, **86** (2006), 331–340. https://doi.org/10.1016/j.sigpro.2005.05.013

23. I. Antoniou, K. Gustafson, Wavelets and stochastic processes, *Math. Comput. Simulat.*, **49** (1999), 81–104. https://doi.org/10.1016/S0378-4754(99)00009-9

24. S. Mendelson, Learnability in Hilbert spaces with reproducing kernels, *J. Complexity*, **18** (2002), 152–170. https://doi.org/10.1006/jcom.2001.0586

25. M. Pontil, A note on different covering numbers in learning theory, *J. Complexity*, **19** (2003), 665–671. https://doi.org/10.1016/S0885-064X(03)00033-5

26. J. Du, M. G. Cui, Solving the forced Duffing equation with integral boundary conditions in the reproducing kernel space, *Int. J. Comput. Math.*, **87** (2010), 2088–2100. https://doi.org/10.1080/00207160802610843

27. Y. Yu, J. Niu, J. Zhang, S. Y. Ning, A reproducing kernel method for nonlinear C-q-fractional IVPs, *Appl. Math. Lett.*, **105** (2022), 107751. https://doi.org/10.1016/j.aml.2021.107751

28. M. Xu, L. Zhang, E. Tohidi, A fourth-order least-squares based reproducing kernel method for one-dimensional elliptic interface problems, *Appl. Numer. Math.*, **162** (2021), 124–136.

29. Y. K. Yu, X. M. Yang, Y. Q. Cui, J. Niu, A broken reproducing kernel method for the multiple interface problems, *Comput. Appl. Math.*, **41** (2022), 260. https://link.springer.com/article/10.1007/s40314-022-01963-7

30. R. Ewing, O. Iliev, R. Lazarov, A modified finite volume approximation of second-order elliptic equations with discontinuous coefficients, *SIAM J. Sci. Comput.*, **23** (2001), 1335–1351. https://doi.org/10.1137/S1064827599353877

31. Z. Zhao, Y. Lin, J. Niu, Convergence order of the reproducing kernel method for solving boundary value problems, *Math. Model. Anal.*, **21** (2016), 466–477. https://doi.org/10.1080/13926292.2016.1205195

AIMS Press